Journal of Materials Chemistry A

ROYAL SOCIETY OF CHEMISTRY

PAPER

View Article Online
View Journal | View Issue

Cite this: J. Mater. Chem. A, 2024, 12, 15278

Performance of environmentally friendly, liquid-infused coatings against biofouling: evaluation of macrofouling and microbially induced corrosion in freshwater environments†

Teresa Walter,[a] Manuela Langbein,[b] Patrik Blenk,[b] Alexander B. Tesler,[c] Lucia H. Prado,[c] Dan Bornstein,[c] Sannakaisa Virtanen,[c] Kathrin Castiglione *[b] and Nicolas Vogel *[a]

Received 31st January 2024
Accepted 26th March 2024

DOI: 10.1039/d4ta00741g

rsc.li/materials-a

Biofouling, caused by the attachment of micro- and macroorganisms, increases the fuel consumption of ships and compromises aquatic infrastructure, especially by microbially induced corrosion. Conventional anti-fouling strategies often rely on the release of toxic substances. Liquid-infused coatings offer an alternative strategy, which has shown promising anti-fouling performance in maritime settings. In this study, we focus on freshwater systems and investigate the performance of a set of recently developed liquid-infused coatings with low environmental impact based on sustainable or non-toxic materials and energy-efficient fabrication. We combine field studies at two freshwater bodies in Bavaria, Germany with laboratory experiments focusing on corrosion and microbial attachment under controlled conditions. Our results indicate that liquid-infused coatings with low environmental impact can show a reduction in general biofouling, mussel attachment, and corrosion rates, as well as the attachment of *Thiobacillus thioparus* and *Pseudomonas fluorescens*, organisms known to cause microbially induced corrosion.

Introduction

Marine biofouling and microbially induced corrosion (MIC) bring about great challenges for global shipping and water infrastructure in both marine and freshwater systems.[1,2] Biofouling is defined as the uncontrolled colonization of submerged surfaces by aquatic species such as microorganisms, micro and macro algae, or small invertebrates, including mussels and barnacles.[3,4] Biofouling negatively impacts industries in different aspects. Increased hydrodynamic resistance, caused by drag forces from the roughened ship hulls, raises fuel consumption and leads to higher emissions and costs for fuel (by up to 40%)[5] as well as time- and resource-consuming cleaning procedures.[4,6,7] Some microorganisms, *e.g.*, sulfate-reducing (SRB), sulfur-oxidizing (SOB), iron-oxidizing (IOB), or iron-reducing (IRB) bacteria, can cause MIC through their biofilms and metabolic products,[8,9] and thus compromise the stability of aquatic infrastructure. Various MIC mechanisms require completely different physical and chemical conditions, but what they have in common is that they either directly or indirectly promote the key reaction in the corrosion of iron-containing metals: $Fe^0 \rightarrow Fe^{2+} + 2e^-$.[10] Commonly, these mechanisms are classified according to the presence of oxygen in a particular environment. Under anaerobic conditions, MIC occurs, for example, through the production of metabolites that enhance the oxidation of Fe^0 to Fe^{2+} by coupling it with the reduction of H^+ to H_2, through electron carriers (H_2 or organic molecules) that shuttle electrons between Fe^0 and microorganisms or *via* direct metal-to-organism electron transfer.[11] In this context, it was only recently shown that electrically conductive pili in *Geobacter sulfurreducens* play a crucial role in direct electron uptake from metallic iron,[12] showing the complex interplay between redox chemistry and microbiology. Under aerobic conditions, on the other hand, MIC is promoted by microbial recycling of Fe^0 oxidants and by formation of biofilms that lead to the generation of low-oxygen environments in their deeper layers that enable the growth of anaerobes such as SRBs.[11] Certain species, such as the aerobic organism *Shewanella oneidensis*, are also capable of direct metal-to-microbe electron exchange.[13] In addition to the economic and safety aspects that arise from the damage to infrastructure elements, biofouling also has an ecological dimension as invasive species are introduced to different ecosystems *via* ships, and can thus suppress indigenous species.[14–19]

[a]Institute of Particle Technology, Friedrich-Alexander-Universität Erlangen-Nürnberg, 91058 Erlangen, Germany. E-mail: nicolas.vogel@fau.de

[b]Institute of Bioprocess Engineering, Friedrich-Alexander-Universität Erlangen-Nürnberg, 91052 Erlangen, Germany. E-mail: kathrin.castiglione@fau.de

[c]Chair of Surface Science and Corrosion, Friedrich-Alexander-Universität Erlangen-Nürnberg, 91058 Erlangen, Germany

† Electronic supplementary information (ESI) available. See DOI: https://doi.org/10.1039/d4ta00741g

Mussels are especially concerning because of their particularly strong adhesion to many substrate materials, mediated by a durable natural glue based on dopa-enriched proteins.[20] No synthetic glue is similarly unaffected by water or turbulent forces.[21] The adhesion mechanism is an interplay of various mussel foot proteins (Mfps), and the strength depends on the curing of the polymer chains in the individual adhesion proteins.[20,22] Thus, the removal of attached organisms is difficult and cost-intensive and the transport to different ecosystems is widespread.

The combination of fouling occurring both at the micro (*i.e.*, bacteria) and macro-scale (*i.e.*, mollusks) complicates the development of effective, broad anti-fouling approaches, as several length scales need to be simultaneously addressed. In the process, both fouling effects can be synergistically reinforced when microorganisms settle on the surface and provide adhesion points for bivalves by shielding the underlying surface chemistry.[23] Thus, effective coating strategies must be able to prevent the adhesion of all fouling organisms.

Initial anti-fouling strategies were based on releasing toxins like tributyltin (TBT).[2] However, as these biocides affect the environment, their application is prohibited in large parts of the world and should be generally avoided. TBT was found to cause severe damage to several aquatic species and thus was banned by the International Maritime Organization in 2008.[24,25] Other chemically active coatings contain, for example, copper or zinc, which can also accumulate in invertebrates such as copepods and amphipods.[26] To avoid such negative environmental impacts, coatings based on physical release mechanisms that prevent the adhesion of biological species without releasing potentially toxic species into the environment have been the focus of research activities.[3,8,27] In the last decade, a new class of surface coatings, *i.e.*, slippery liquid-infused porous surfaces (SLIPSs), emerged with promising anti-fouling capacities at all length scales,[28–32] and significantly reduced adhesion strengths.[32–36] SLIPS coatings operate by confining a thin film of a fluid lubricant within porous surface structures. If the involved interfacial energies are properly controlled,[28,37–39] this liquid film is not replaced by a contaminating fluid or solid and thus shields the surface against the adhesion of liquids, contaminants, or organisms.[31,36,37,40–42] Different variations of this strategy replace the underlying porous substrate with organogels,[30,33,35,43] or grafted, liquid-like molecules.[44–46]

To this point, field studies underlined the performance of SLIPS coatings against biofouling, but have predominantly explored marine environments,[32,34–36] while freshwater scenarios remain underexplored.[33] While the shipping industry may be primarily affected by marine biofouling, freshwater systems host important water infrastructure, including floodgates, weirs, hydropower plants, and bridges. Freshwater infrastructure may be less prone to corrosion compared to chloride ion-rich sea water, but microbially induced corrosion and macrofouling can compromise the operation of such infrastructure and thus cause safety concerns. Therefore, an evaluation of the performance of liquid-infused coatings against biofouling in freshwater environments is important. A critical aspect to be considered when developing anti-fouling coatings to be used in freshwater infrastructure is the environmental impact, as such water bodies are often directly connected to drinking water supplies. These concerns have led to a more restrictive regulation of coatings to prevent the release of fluorinated or potentially harmful substances.

In this article, we explore the performance of a set of recently developed, environmentally friendly liquid-infused coatings based on sustainable or non-toxic materials against biofouling in German freshwater reservoirs. The coating processes are scalable, have a low environmental impact, and are fabricated with low energy consumption.[47–50] We combine two field studies at different locations. Using a well-accessible lake at Tiergarten Nuremberg, Germany enables us to conduct a time-resolved study on general biofouling. At lake Roth (Rothsee), Bavaria, Germany, we explore the long-term performance of the coatings that were continuously submerged within the water body. This lake has been facing problems with the invasive species *Dreissena polymorpha* (zebra mussel) and *Dreissena rostiformis bugensis* (quagga mussel) for years and thus provides the perfect ecosystem to study the combined effects of fouling at all length scales. Additionally, we perform laboratory studies on electrochemical corrosion and the fouling of microorganisms known to induce microbial corrosion to give a more detailed insight into the protective properties of the tested coatings for biofouling-related applications.

Experimental

Preparation of self-cleaning surfaces

Throughout this work, several slippery surface coatings that were recently developed in our laboratory and showed promising liquid repellency properties, *i.e.*, infused poly(butyl methacrylate) (*ipBMA*),[50] infused tung oil-based coatings with silicon oil as a lubricant (*iTuSi*),[48] infused tung oil-based coatings with sunflower oil as a lubricant (*iTuSu*),[48] infused, functionalized polydopamine coatings (*fpDa*),[47] infused poly(dimethylsiloxane) (*iPDMS*),[32] and infused UV-cured polydimethylsiloxane (*iUV-PDMS*),[49] were tested, for which the preparation procedures are described in the following.

Preparation of *ipBMA*, *iTuSi*, and *iTuSu* coatings. The coatings based on 1-droplet systems were prepared following procedures by Walter *et al.*[50] and Dehm *et al.*[48] Briefly, the coating systems were prepared with 0.2 g poly(butyl methacrylate) (pBMA, synthesized *via* miniemulsion polymerization from butyl methacrylate, 99%, Sigma Aldrich) or tung oil (100% pure tung oil, Uulki, Belgium) as binder and 0.4 g hydrophobic fumed silica particles (Aerosil R805, Evonik). The components were dissolved and dispersed in 6 g *tert*-butyl acetate (*t*ButAc, ≥99%, Merck KGaA). Afterward, 24 g of a sodium dodecyl sulfate (SDS, ≥99%, Carl Roth) solution in ultrapure water (3.2 g L^{-1}) was added and the mixture was ultrasonicated under ice-cooling for 180 s at 90% amplitude (Sonifier 450D, Branson, 1/2″ tip) to form stable microdroplets in water.

Next, superhydrophobic coatings were applied on polycarbonate or black carbon steel (S355J2+N according to DIN EN 10025-2), cleaned by ultrasonication in ethanol (99.5% denaturated, Carl Roth) and water. The coatings were applied with

a spray gun (Evolution Silverline Two in One, Harder & Steenbeck). Each coating was sprayed three times with a 30 s drying time in between each cycle to coat the substrates sufficiently and achieve superhydrophobicity. The spray nozzle was placed 15 cm from the substrate. After the coating process was completed, the samples were dried horizontally at room temperature. In the case of the coatings containing tung oil, an additional UV treatment (Bio-Link 365, Vilber, $\lambda = 365$ nm) of 6 h was applied to fully cure the binding material. Also, a primer layer was applied underneath the coating by spraying pure tung oil and cured for 1 h before applying the coating system, as this has been shown to increase the adhesion to the substrate and avoid delamination.[48] Subsequently, the coated slides were washed by immersion in deionized water.

To form the slippery liquid-infused porous surfaces the superhydrophobic coatings were infiltrated using silicone (*ipBMA*, *iTuSi*) with a viscosity of 10 cSt or sunflower oil (*iTuSu*) with a viscosity between 60 and 70 cSt by spraying the respective oil on top of the coating three times.

All coatings were visually examined to ensure that they were uniform and characterized concerning their wetting properties *via* the contact angle before and after infiltration with the lubricant (to ensure superhydrophobic properties), and by contact angle hysteresis and sliding angles after infiltration with the lubricant. To provide quality control for all coatings used in this study, we used the established and published coating procedures in our lab (shown in ESI Fig. SI1†),[47–50] determined reference values for all wetting parameters (contact angle, contact angle hysteresis, and sliding angles), which are listed in Table SI1,† and only used coatings that had parameters with the following deviations from these reference data: contact angle of non-infused surfaces: less than 7° deviation from the reference value; contact angle hysteresis: less than 3° deviation from the reference value; sliding angles: less than 3° deviation from the reference value.

Preparation of *fpDa* coatings. The liquid-infused coatings were prepared following protocols for a one-step[46] and an environmentally more benign two-step[47] approach that avoids the use of organic solvents on different materials (glass, black carbon steel, polycarbonate). The substrates were cleaned by ultrasonication in ethanol and water and pre-treated with oxygen plasma for 5 min at 10 sccm oxygen flow and 100 W plasma power.

For the two-step approach, the samples were first coated with a polydopamine (pDa) coating. This step was performed as follows. An aqueous solution containing 1 g L^{-1} dopamine HCl (≥98%, Sigma-Aldrich) and 10 mM tris(hydroxymethyl)aminomethane (TRIS, ≥99.9%, Carl Roth) was prepared and the samples were immersed with stirring at 900 rpm for 24 h. Afterward, the samples were rinsed with water and dried at room temperature. In a second step, the pDa-layer was functionalized for at least 48 h by adding silicone oil (15 μL cm^{-2}) containing 20 mM monoaminopropyl-terminated polydimethylsiloxane (MAP-PDMS, MCR-A11, >95%, Gelest Inc.) and 20 mM triethylamine (TEA, 99%, Sigma Aldrich). In the course of this time, the MAP-PDMS reacts with the pDa coating to functionalize the surface *in situ* and thus hold the inert silicone oil layer in place.

The one-step approach was based on spray-coating a reactant mixture on the samples, which was then allowed to react for 96 h at room temperature. The mixture was prepared by first dissolving 0.04 g dopamine HCl in 40 mL tetrahydrofuran (THF, 99.9%, Carl Roth) and methanol (MeOH, ≥99.5%, Carl Roth) at a ratio of 1 : 1 by volume. Next, 20 mM TEA, 20 mM MAP-PDMS, and 100 mM silicone oil were added. The reaction mixture was applied in seven spray cycles using a manual spray bottle at a 15 cm distance, 45° inclination, and with a 30 s pause in between the cycles.

Preparation of *iPDMS* coatings. *iPDMS* samples were prepared on glass and polycarbonate substrates, which were cleaned by ultrasonication in ethanol and water and pre-treated with oxygen plasma for 5 min at 10 sccm oxygen flow and 100 W plasma power. Following a modified protocol by Amini *et al.*[32] a Dowsil™ Sylgard 184 elastomer kit (Dow, Inc., Midland, US) was used, and the base and curing agent were mixed thoroughly in a 10 : 1 ratio before being applied to the substrate (0.05 g cm^{-2}) and distributed with a spatula. After curing for 4 h at 80 °C the PDMS was infused with excess silicone oil (viscosity of 10 cSt) for at least 48 h before using further.

Preparation of *iUV-PDMS*. The *iUV-PDMS* coatings were prepared on glass and black carbon steel substrates following an adapted procedure by Tesler *et al.*[49] The surfaces were cleaned by ultrasonication in acetone (Carl Roth) and ethanol for 10 min and afterward horizontally placed into a Petri dish under a quartz cover. Approximately 20 μL cm^{-2} silicone oil (500 cSt, Carl Roth) was dropped to cover the entire sample surface and uniform coverage was achieved by tilting the sample. Last, the samples were illuminated for 1 h using a medium-pressure ultraviolet (UV) mercury (Hg) lamp at 1 kW (UVAPRINT HPV, Hoenle AG, Germany) at a working distance of ~20 cm between the lamp and substrate.

Biofouling study

The anti-biofouling performance of the different coatings was tested in two field studies during fall 2021 and 2022, in which the extent of biofouling on the surfaces was observed. To this end, 15 × 15 cm substrates (glass, polycarbonate) were coated with the different systems in triplicate. The backside of the glass substrates was coated with white VC Tar 2 (International) or light grey car paint (Nigrin) to exclude visible fouling on the non-coated backside. The samples were mounted in self-built frames and put into a pond at the zoo in Nuremberg, Germany for 12 weeks. To exclude any site-specific influences the samples were randomly ordered across all frames. The frames were placed vertically at a depth of 50 cm on stilts and fixed to the border of the pond using tent pegs. The position of the samples was chosen to allow simple access to the samples from the shoreline and sufficient immersion to ensure continuous immersion during the field study. They were placed at the northwest shoreline of the pond facing the course of the sun from southeast. To observe the biofouling, the samples were shortly removed from the water every two weeks and a picture of

each coating was taken at constant lighting using a self-built photobox equipped with a camera (Sony), a softbox (Godox) and a flash (V1S, Godox). The images were evaluated using ImageJ by cropping the borders off at 1 cm, setting it to default and a threshold of 60 to determine the coverage with fouling species by evaluating black pixels per image.

Macrofouling by zebra and quagga mussels

The performance of the different coatings against macro fouling was tested in a field study during the summer and fall of 2022 at lake Roth, Bavaria, Germany, in which the adhesion of *Dreissena polymorpha* and *Dreissena rostiformis bugensis* on the surfaces was observed. 15 × 15 cm substrates (black carbon steel) were coated with the different systems in triplicate. The backside of the steel was coated with white VC Tar 2 (International) to protect the material from corrosion. The samples were mounted in self-built frames and put into the nature reserve of lake Roth for four months. To exclude any site-specific influences the samples were randomly ordered across all frames. The frames were placed vertically at a depth of 3 m hanging on a swimming platform anchored to the bottom of the lake. To observe the biofouling, the samples were removed from the water after four months and a picture of each coating was taken at constant lighting using a self-built photobox equipped with a Camera (Sony), a softbox (Godox), and a flash (V1S, Godox). The mussels on the samples were counted using ImageJ.

Electrochemical corrosion measurements

The coatings' resistance to electrochemical corrosion was tested on black carbon steel samples (3 × 5 cm) non-coated and coated with the different slippery systems. The bare steel samples were cleaned in acetone and ethanol in an ultrasonic bath for 10 min each prior to electrochemical measurements. The experiments were performed in a 0.1 N sodium chloride (NaCl, >99.8%, Carl ROTH) electrolyte and a three-electrode configuration. The respective sample was connected as the working electrode, with a platinum electrode as the counter electrode, and a reversible hydrogen electrode as the reference electrode. The coatings were in contact with the electrolyte through a circular opening with a diameter of 2 cm sealed by an O-ring (12.6 cm^2). Open-circuit potential (OCP) measurements were conducted until reaching a stable value (Zahner Zennium electrochemical workstation). Subsequently, potentiodynamic polarization was performed at room temperature from −300 mV with respect to OCP up to 2 V in the anodic direction at a 1 mV s^{-1} scanning rate. The corrosion inhibition efficiency (IE) was calculated as follows:

$$\mathrm{IE} = \left(\frac{I_{\mathrm{corr},0} - I_{\mathrm{corr,c}}}{I_{\mathrm{corr},0}}\right) \times 100\%$$

where $I_{\mathrm{corr},0}$ is the corrosion current density of the uncoated sample and $I_{\mathrm{corr,c}}$ is the corrosion current density of the coated sample. The values were obtained after the polarization experiments using the Tafel method by extrapolation of the anodic and cathodic current densities at ±50 mV from the OCP.

Laboratory study on corrosion-inducing microorganisms

Bacteria and growth conditions. Two aerobic bacteria were used as model microorganisms for biofilm formation and analysis: *Pseudomonas fluorescens* strain DSM 50090 and *Thiobacillus thioparus* strain DSM 505. Both bacteria were obtained from the German Collection of Microorganisms and Cell Cultures (DSMZ, Braunschweig, Germany). The cells were cultured at 30 °C, either in Tryptone Soya Broth (TSB) medium (*P. fluorescens*) or in 290 S6 medium (*T. thioparus*). Optical density (OD) was measured at 600 nm in the case of *P. fluorescens* or at 500 nm in the case of *T. thioparus*. For OD_{500} measurement, cells were washed with phosphate buffered saline (PBS) by centrifugation at 16 000*g* for 10 min at room temperature to avoid interference from media components at this wavelength.[51]

Biofilm experiments and quantification. Biofilm experiments were done in triplicate with steel coupons (2.5 × 3 cm) as model surfaces. Prior to setting up an experiment, coupons were sterilized with UV light (100 000 mJ cm^{-2}) in a UV crosslinker (UVLink 1000, Analytik Jena). Experiments were performed in 200 mL Erlenmeyer flasks with 40 mL medium. OD was adjusted to an initial start OD of 0.1. All incubation steps with steel coupons were performed without shaking. Cultivation time with coupons was 4 days for *P. fluorescens* and 12 days for *T. thioparus* reflecting their differences in growth rates. The medium was then carefully removed and the coupons were gently washed once with the medium to clear them from non-adherent cells. Afterward, the biofilm was detached from the coupons by rinsing with 4 mL of medium using a pipette and transferred into Falcon tubes.

Dividing bacteria were quantified by determination of colony forming units (CFU) on TSB agar plates in the case of *P. fluorescens* or on 290 S6 agar plates in the case of *T. thioparus*. For this purpose, plates containing 15 g L^{-1} agar were inoculated with serial dilutions of bacterial biofilm and incubated at 30 °C for two 2 or 10 days, respectively. After this time, colonies were counted, and CFU mL^{-1} was calculated. The statistical significance of observed differences in biofilm formation between the reference and coated samples was determined using an unpaired *t*-test for equal variances.

Results and discussion

Preparation of environmentally friendly slippery coatings

For this study, we selected different liquid-infused coatings with low environmental impact that were developed in recent years in our laboratories.[47–50] All coatings are prepared from aqueous dispersions, avoiding the excessive use of organic solvents, and applied at room temperature to minimize energy consumption. The selection includes coatings representing the three general strategies to create liquid-infused coatings, *i.e.*, SLIPSs, organogels, and grafted liquid-like molecules.[52]

The first set of coatings includes three types of environmentally benign SLIPS coatings, formed from aqueous dispersions of a polymeric binder and hydrophobic silica particles. Together, these components form the porous structure into

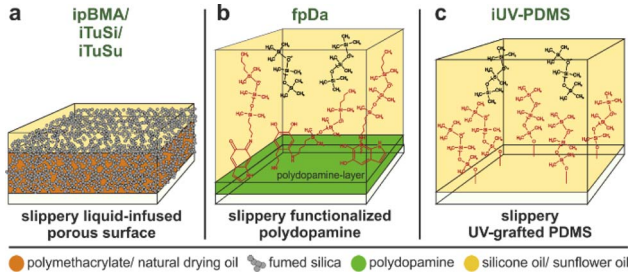

Fig. 1 Schematic illustration of the different environmentally friendly slippery coatings included in this study. (a) Liquid-infused porous surfaces based on polymethacrylates (*ipBMA*) or natural drying oils (*iTuSi*/*iTuSu*) as a polymeric binder, fumed silica as a structuring component, and silicone oil (*ipBMA*/*iTuSi*) or sunflower oil (*iTuSu*) as a lubricant. (b) Silicone oil-infused functionalized polydopamine coating (*fpDa*). (c) Silicone oil-infused UV-grafted polydimethylsiloxane (*iUV-PDMS*) coating.

which the fluid lubricant is infused (Fig. 1a). The three samples differ in their components. Infused poly(butyl methacrylate) (*ipBMA*) coatings use silicone oil as the lubricant and constitute all-synthetic coatings.[50] The polymeric binder can be replaced by naturally occurring tung oil (Tu), which is infused with silicone oil (Si) to form the liquid-infused *iTuSi* coatings.[48] In this case, a first primer layer of pure tung oil was added to improve the incorporation of the silica particles and the substrate adhesion.[48] Replacing synthetic silicone oil as the lubricant with natural sunflower oil (Su) forms the fully renewable *iTuSu* coating.[48] Detailed schematics of the fabrication of these coatings are shown in Fig. SI1a,† and the development, optimization, and characterization of all coatings are reported in previous publications.[48,50]

The second set of coatings represents the class of infused, grafted liquid-like molecules, and consists of immobilized polydimethylsiloxane (PDMS) chains that are bound to the underlying surface to match the chemical nature of silicone oil used as the lubricant. Infused, functionalized polydopamine coatings (*fpDa*) take advantage of a pDa base layer, which is functionalized with monoaminopropyl-terminated polydimethylsiloxane chains to minimize the interfacial tension with silicone oil.[47] Infused, UV-grafted PDMS (*iUV-PDMS*) is fabricated by irradiating a thin fluid silicone oil film to covalently anchor PDMS chains to the underlying surface.[49] The detailed fabrication processes are shown in Fig. SI1b and c,† and coating process details and characterizations are reported in our previous publications.[47,49]

As a representative of the last class of liquid-infused coatings, we included silicone oil-infused PDMS (*iPDMS*) as an organogel widely used as a liquid-infused repellent coating,[30,35,53] with a demonstrated performance against marine biofouling.[32,35]

For this study, we chose polycarbonate (PC) and black carbon steel (S355J2+N according to DIN EN 10025-2) as two relevant, but chemically different substrate materials. PC is often used *e.g.* in boat hulls, while carbon steel is the material used in pipes, and Bavarian aquatic infrastructure, such as pipes, rakes, floodgates, and weirs.

Biofouling in freshwater lakes

We assessed the performance of all coatings against biofouling in freshwater bodies in two field studies. The first study was performed for three months during fall 2022 at a pond at Tiergarten Nuremberg, Germany. This pond was well accessible and allowed a time-resolved study of biofouling, especially with algae. For this study, we chose PC substrates (15 × 15 cm) and used all coatings in triplicate. The samples were randomly placed into holders, which were anchored vertically within the pond at a depth of 50 cm (Fig. SI2a†). Biofouling was investigated every two weeks by removing the samples from the water and taking images while ensuring identical light conditions. Fig. 2 summarizes the results of this time-resolved study.

Fig. 2a exemplarily shows photographs of two representative samples throughout the field study. The uncoated PC reference (top row) experienced significant fouling already in week 4, which densified in the course of the study and completely covered the entire substrate. The infused poly(butyl methacrylate)-based SLIPS coating (*ipBMA*; bottom row), however, showed a much lower fouling coverage compared to the uncoated reference.

We quantitatively compared the biofouling of all tested samples by image analysis of the photographs taken every two weeks to determine the degree of coverage. Fig. 2b shows the evolution of biofouling determined from this image analysis. The *ipBMA* coatings outperformed the other environmentally friendly coatings and decreased the fouling by almost 80% compared to the uncoated reference. Similar trends were also found for coatings on glass substrates in a preliminary study in the fall of 2021 (Fig. SI3a and c†), underlining the broad adhesion of the *ipBMA* coating on different surfaces. A good performance was also observed for the *iUV-PDMS* coatings which reduced the fouling by 50% after week 12 (Fig. SI3b and d†), albeit only on glass substrates since it was not possible to coat PC substrates due to insufficient hydroxy groups on the polymeric substrate.

The *iPDMS* and *iTuSi* coatings showed a reduction in biofouling compared to the reference until week six, while afterward, the fouling increased drastically (Fig. 2b). In the case of the *iPDMS*, which has been shown to be very effective against marine biofouling,[32] the loss of performance could be tracked to a detachment of the PDMS film from the underlying substrate. In a reference experiment included in this study, we used a glass substrate, where the adhesion to the PDMS layer is known to be better,[32] and found *iPDMS* being efficient against biofouling (Fig. SI3a and c†), in agreement with reports in the literature on marine biofouling.[32] Both the sunflower-oil-infused *iTuSu* coating and the functionalized polydopamine-based coating *fpDa* failed already after two weeks and showed comparable biofouling as the uncoated reference.

When comparing the three SLIPS-based coatings, we note that all coatings initially showed a large reduction in biofouling but eventually failed in their performance over time. *ipBMA* showed the best performance and only exhibited an onset of biofouling at the last time points of the study, while *iTuSi* showed a decreased performance from week 8, and *iTuSu*

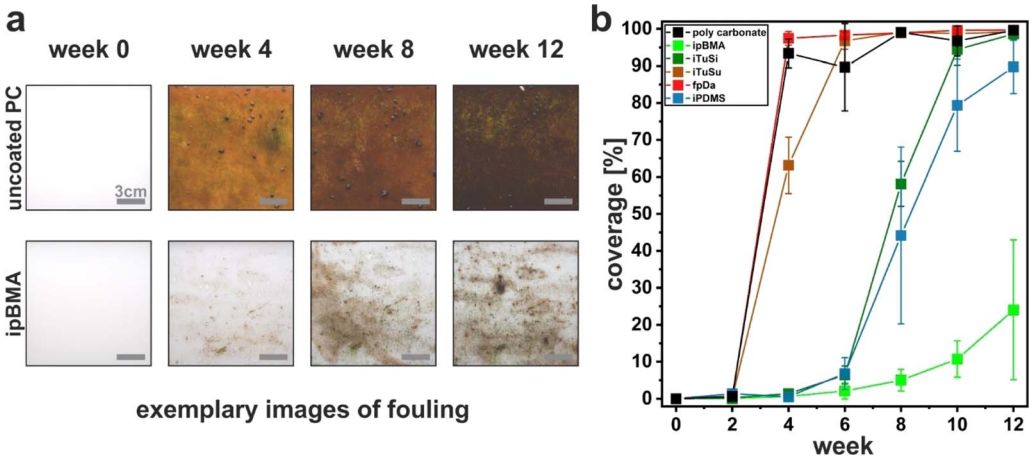

Fig. 2 Biofouling of coated polycarbonate substrates immersed in a pond at Tiergarten Nuremberg, Germany in fall 2022. (a) Exemplary images of the fouling development on an uncoated reference (polycarbonate, upper row), and an *ipBMA* sample (bottom row) before and after 4, 8, and 12 weeks of immersion. (b) Quantification of biofouling *via* image analysis of substrate coverage of all tested coatings.

already failed after 4 weeks. While the exact origin of the failure cannot be determined from this study, we note that during this time-resolved study, the substrates were removed from the water at regular intervals to image and quantify the fouling process. This removal from the water phase induces a drying step and the creation of a three-phase contact line between the lubricated surface, water, and air associated with the meniscus of the water film receding from the surface. It has been shown in the literature that such three-phase contact lines deform the lubricant film, which forms wetting ridges along the water surface.[54–56] These wetting ridges have been shown to be a major source of lubricant depletion, which is sheared off along with the meniscus of the receding water phase.[57,58] Notably, this loss mechanism is enforced by the design of this field study by the periodic removal of the substrates. In these challenging conditions, the ability to retain the lubricant in these scenarios was highest for *ipBMA*, followed by *iTuSi* and *iTuSu*, which correlates with the decreasing hydrophobicity of the components of these coatings.[48] This correlation suggests that the interfacial energies, which are tailored by matching the hydrophobicity of the surface texture and lubricant, can influence this physical removal of the lubricant. Following this hypothesis, an improved performance can be expected for an experimental design with a continuous submersion, as we will discuss below. Similar to the case of *ipBMA*, the *iTuSi* coating showed the same performance when coated on glass, again underlining the versatility of the coating process with respect to the underlying substrate (Fig. SI3e†). Lastly, despite efficient repellency properties under laboratory conditions,[47] the *fpDa* coating showed no fouling decrease compared to the uncoated reference. We note however, that a chemically similar coating, prepared in a one-step process involving organic solvents,[46] showed a decrease in biofouling of approximately 80% compared to an uncoated reference (Fig. SI3a and c†). In this case, the transfer to an environmentally benign approach was not successful against biofouling.

Fouling with *Dreissena* species

Complementing the investigations of biofouling in freshwater systems, we evaluated the coatings in a second field study in the summer and fall of 2022 in lake Roth (Rothsee), Bavaria, Germany. This lake was chosen since it has a known population of intrusive *Dreissena polymorpha* and *Dreissena rostiformis bugensis* species with a large detrimental impact on the water infrastructure in this lake. In this study, we used carbon steel substrates (15 × 15 cm panels). Due to limitations in available space, we excluded *iPDMS* and *iTuSu* in this study since they showed poor performance in the first study. The substrates were attached at a water depth of 3 m to a platform anchored in the center of the lake (Fig. SI2b†). After four months of continuous immersion (Nov. 2022), we removed the substrates and characterized the biofouling by image analysis, and, in particular, by counting the number of settled *Dreissena* mussel species (Fig. 3).

We first qualitatively evaluated the general biofouling from photographs taken at the end of the four-month immersion. Note that due to the dark color of the steel panels, a quantitative image analysis as in the time-resolved study at the Tiergarten pond (Fig. 2) was not possible. Fig. 3 a shows that the uncoated, bare steel reference exhibited pronounced biofouling. Fig. 3b shows exemplary photographs of the different environmentally friendly liquid-infused coatings. A decrease in fouling compared to the uncoated reference was seen for *ipBMA* and *iTuSi* but not for *iUV-PDMS* and *fpDa*, again in qualitative agreement with the study on PC substrates at the Tiergarten pond (Fig. 2).

Additionally, we found areas with evenly distributed mussels or the formation of mussel colonies on all *fpDa*, *iUV-PDMS*, and uncoated reference samples (Fig. 3a and b). We quantified this macrofouling based on mussel attachment by manually counting *Dreissena* mussels on all substrates (Fig. 3c). This quantification supports the qualitative impression of the samples. Firstly, the number of mussels attached to the *fpDa*

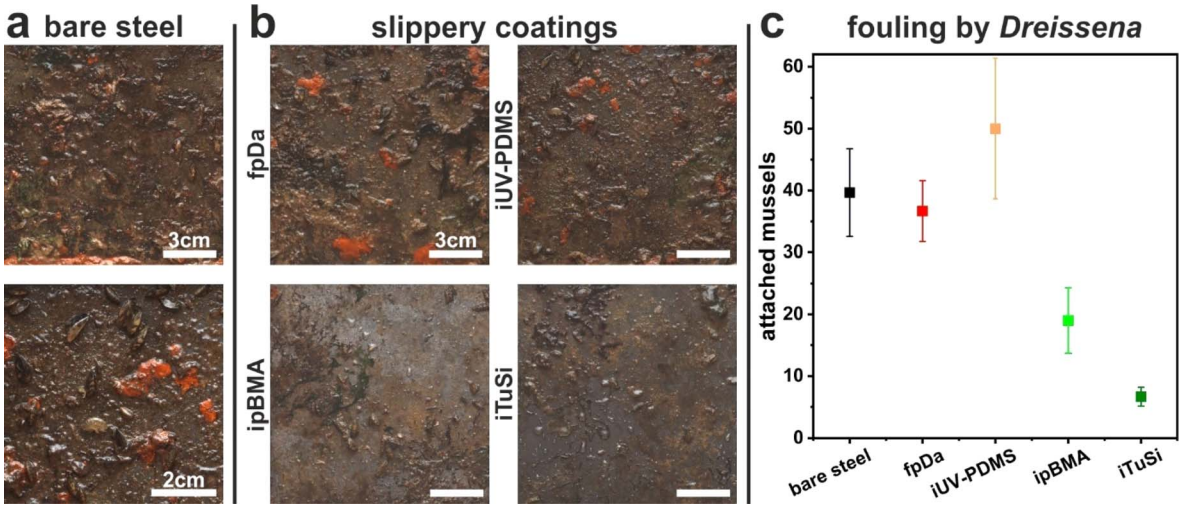

Fig. 3 Biofouling on uncoated and coated steel samples during a field study in summer/fall 2022 at lake Roth, Germany. (a) Exemplary photographs of biofouling on uncoated carbon steel as a reference after four months. (b) Exemplary photographs of the biofouling on different environmentally benign liquid-infused coatings. All scale bars correspond to 3 cm. (c) Average number of attached mussels (*Dreissena polymorpha*/*Dreissena burgensis*) on the different samples.

substrate was in the same range as the number on the uncoated carbon steel substrate. *iUV-PDMS* showed even slightly higher numbers, indicating that these coatings did not prevent macrofouling. The number of mussels counted on the *ipBMA* substrates was approximately half of the count on the uncoated reference, showing an anti-fouling performance of this coating. The lowest numbers were found on the *iTuSi* coatings, with a reduction of ~85% with respect to the uncoated reference. As hypothesized above, the improved performance of the *iTuSi* sample may be attributed to the continuous immersion in this study. In addition, this sample was also prepared using a tung oil primer layer to improve the integration and adhesion of the silica particles forming the porous support.[48] Notably, despite a comparable overall coating thickness (~2–3 μm)[48,50] this primer layer may further protect the coating against fouling, compared to the *ipBMA* coating, either by partial swelling with silicone oil or by providing an enhanced physical barrier.

Summarizing both field studies, the environmentally friendly SLIPS coatings exhibited significant reductions of biofouling, which depended on environmental boundary conditions such as the removal from the water phase. Best performances were found for continuous immersion, where the developed SLIPS coatings provided efficient resistance to fouling even over extended periods of time. These coatings showed similar performances on all tested substrate materials. Liquid-infused coatings based on surface functionalization with silicone oil chains did not provide an efficient reduction of biofouling, except UV-PDMS coated on glass substrates. Our results align well with previous studies on lubricant-infused surfaces in different scenarios. These studies demonstrated that loss of lubricant mediated by liquid menisci is difficult to avoid and can lead to degradation of performance.[55,57] When submerged in water, however, these studies showed the ability of liquid-infused coatings to retain repellent and self-cleaning properties over extended periods of time or large water volumes, for example in preventing protein adsorption[59] or marine biofouling.[32]

Electrochemical corrosion

As carbon steel is a widely used material in aquatic infrastructure, the fundamental corrosion behavior of coated steel was investigated in a laboratory setting under controlled conditions to complement the real-world corrosion detected in the field studies. After the four months of incubation in lake Roth, corroded spots on the reference steel panel and the panels coated with *fpDa* and *iUV-PDMS* were found, while none of the other samples showed any visible signs of corrosion. Corrosion of uncoated carbon steel is expected to occur under exposure to natural waters, hence non-occurrence of visible corrosion after 4 months of immersion demonstrates good corrosion protection by most of the coatings studied here. It has been previously shown that liquid-infused coatings can be effective against corrosion,[3,27,60] but this effect may be compromised in long-term exposures by loss of lubricant.

In addition to corrosion observations from field studies, we investigated the corrosion protection ability of the different coatings *via* standard potentiodynamic polarization measurements in a 0.1 N sodium chloride solution (Fig. 4a). Since such electrochemical characterization requires sufficient conductivity of the electrolyte, the use of similar freshwater as in the field studies is not possible in our electrochemical experiments. We therefore chose controlled conditions with a fixed concentration of 0.1 M NaCl, an electrolyte that is present in natural waters, albeit at lower concentrations in the case of freshwater. The use of this more aggressive electrolyte also allows us to probe corrosion in shorter times compared to the field study, and therefore facilitates the detection of differences and the comparison between the involved samples with a diverse coating structure.

The polarization curve of the bare steel sample shows active dissolution, observable by a continuous increase of the current density in the anodic branch. At high anodic current densities, a diffusion-controlled regime is reached. For all coated samples, significantly lower anodic current densities can be observed, especially under moderate anodic polarization. This indicates that all coatings provide substantial corrosion protection, with notable differences in the first anodic current density plateau (indicating different barrier properties of the different coatings). The polarization curves moreover indicate that corrosion protection of the studied coatings is mostly provided by blocking the anodic metal dissolution reaction (as only minor decreases in the cathodic current densities are observed for the coated samples). It is noteworthy that for all coated samples, a steep increase of the anodic current densities occurs at approximately 0.375 V indicating a loss of the protective properties of the coatings – in agreement with previous observations for similar coatings.[60] A second current increase is caused by oxygen evolution starting at 1.23 V (onset potential for water oxidation). To directly compare the corrosion protection efficiency of the different coatings under free corrosion conditions, the inhibition efficiency was calculated from the i_{corr} values obtained from the polarization curves (as explained in the Experimental section). All coatings suppressed corrosion to some extent with the highest indicated corrosion inhibition efficiency (IE) of 95.6% for the *iTuSi* coating which showed a decrease in its corrosion current density I_{corr} by more than one order of magnitude. The lowest IEs of 75.3% and 76.8% were found with *iTuSu* and *iUV-PDMS* coatings, respectively. The *ipBMA* and *fpDa* coatings both showed an intermediate IE with 86.2 and 80.9%, respectively. The *iUV-PDMS* coating reached similar current densities to those of the uncoated reference at a potential of approximately 0.48 V, indicating that the coating detached or disintegrated at these voltages. At approximately 1.75 V the *fpDa* coating also reached the current density of the bare steel sample, indicating failure or decomposition of the coating. In both cases, defects within the coatings may also serve as attacking sites for chloride ions and the onset of pitting corrosion. As *iUV-PDMS* successfully prevented corrosion in previous studies[49,60,61] we suspect that the lower amount of surface hydroxy groups on carbon steel may prevent a thorough anchoring of the PDMS chains in the process, compromising the quality of this type of coating on steel. Noteworthily, all other coated samples showed a reduced current density compared to the uncoated reference throughout the entire potential range probed in the experiment. Photographs of all samples after the potentiodynamic polarization support this interpretation (Fig. 4 d): *iUV-PDMS* and *fpDa* samples exposed to potentials of 2 V showed clear signs of corrosion which were comparable to those of bare black steel, even though corrosion occurs at a defective site only, whereas a *fpDa* sample exposed to only 1 V did not show any visible corrosion and retained its repellency properties. Samples coated with *ipBMA*, *iTuSu*, and *iTuSi* did not show macroscopic corrosion upon exposure to potentials up to 2 V and retained their repellency (Fig. 4d). When investigating the polarization curves in detail, spikes with higher current densities which rapidly decrease to lower current densities can be seen. We hypothesize that these spikes originate from localized attacks of chloride ions initiating pitting corrosion.[62] Due to the self-healing effect of the liquid-infused coatings such localized corrosion initiation events were suppressed rapidly, recovering the lower current density. Microscopic examinations of the liquid-infused coatings after polarization gave direct evidence of such pitting corrosion (Fig. 4c).

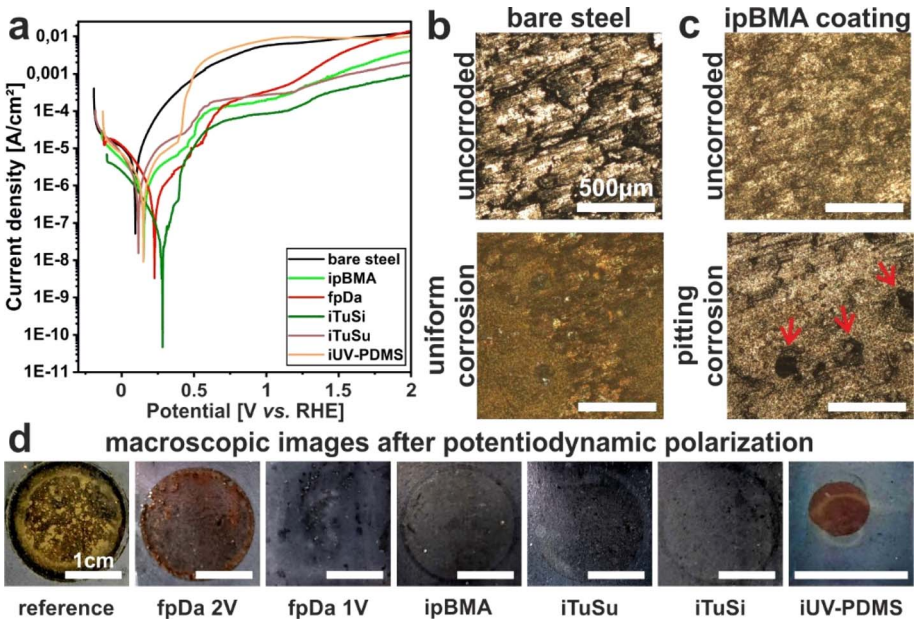

Fig. 4 Corrosion behavior of carbon steel with different liquid-infused coatings in 0.1 N NaCl electrolyte. (a) Potentiodynamic polarization curves (potential plotted against RHE). (b and c) Microscopic investigation of the resultant corrosion behavior. All scale bars are 500 µm. (d) Photographs of the different samples after the potentiodynamic polarization. All scale bars are 1 cm.

Summarizing these experiments, all our developed, environmentally friendly liquid-infused coatings can suppress corrosion of carbon steel under mild conditions. The most effective corrosion resistance was achieved by the tung oil-based *iTuSi* coating. This increased performance, also compared to that of the synthetic, poly(butyl methacrylate) coating, may be caused by the properties of the polymer itself or the presence of a primer layer of bare tung oil that was incorporated in the coating.

The electrochemical corrosion studies do not provide information on the long-term protection ability of the coatings, and the possible influence of microbes present in natural waters on the corrosion performance is ignored in the simplified electrochemical investigations under laboratory conditions. Therefore, corrosion rates determined by long-term immersion experiments in field studies are not expected to be identical to corrosion rates determined by electrochemical measurements on freshly coated samples. However, electrochemical measurements are helpful for fast screening of the performance of the different coatings in comparison, and in addition reveal details on the origin of the observed corrosion protection effects (*e.g.*, blocking of metal oxidation/dissolution *vs.* deceleration of reduction reactions).

Laboratory studies of bacterial attachment using model microorganisms known to be involved in MIC phenomena

While electrochemical corrosion is directly related to the ability of the corroding electrolyte (with aggressive ions) to reach the surface, MIC is a more complex, multistage process that requires the attachment of microorganisms to the surface, the formation of a biofilm, and the subsequent corrosion, *e.g.* as a result of metabolic products produced from organisms within this biofilm.[8] In addition, multiple microorganisms are known to form synergistic communities with complex interactions that can cause more severe MIC phenomena.[8,63,64] The field studies have shown an efficient prevention of corrosion on most coated surfaces (see above), corroborated by an increased resistance to electrochemical corrosion in laboratory tests. To assess whether MIC phenomena can also be reduced by the liquid-infused coatings, we reduced the complexity of the process and focused on the initial step, the attachment of relevant microorganisms to the different surfaces. To this end, we chose *P. fluorescens* and *T. thioparus*, two aerobic organisms with a known involvement in MIC.[65,66] This choice was motivated by the position of our substrates in the field studies in near-surface regions with plenty of access to oxygen. During the initial colonization of the metal surfaces, a thick film of aerobic organisms must first form before anaerobic organisms can also grow in oxygen-depleted zones in its deeper layers near the metal–biofilm interface.[11] Since the growth of the anaerobes is thus substantially influenced by the presence of aerobic organisms and their metabolism, including their extracellular polymeric substances, we have limited our model studies to the initial steps of biofilm formation by two oxygen-dependent microorganisms, which is a necessary first step in the evolution of a more complex, multicomponent MIC-active biofilm. Whereas *T. thioparus* is a sulfur-oxidizing bacterium (SOB),[66] *P. fluorescens* is an Mn^{2+} oxidizing bacterium (MOB),[67] and both constitute important groups of corrosion-causing bacteria[68] typically co-existing with many other microorganisms in a natural biofilm structure. Focusing on the formation of biofilms of single species thus represents a severe reduction in complexity that does not directly investigate the amount of actual corrosion produced by the formed biofilms, nor does it focus on synergies between multiple organisms or the effect of anaerobic conditions likely to occur in closed pipes. The goal of this study therefore is a more general assessment of the role of surface properties in controlling microbial attachment.

For quantitative analysis of biofilms, there are several methods with individual advantages and challenges.[69] In this study, a CFU mL^{-1} assay was used to quantify the number of cells of *P. fluorescens* and *T. thioparus* attached to steel coupons after growth periods of 4 and 12 days, respectively. This assay, also referred to as divisible cell counting, is based on the separation of individual cells on agar plates, which then grow into colonies that are visible without the aid of additional dyes or equipment. For this purpose, the biofilms were detached from the coupons by rinsing them with a specific volume of liquid. The cell suspensions were then plated out on agar plates at various dilution levels and analyzed.

As can be seen in Fig. 5a, all coated samples showed at least an 80% reduction in biofilm formation of *T. thioparus* compared to the uncoated reference samples. All reductions were statistically significant ($p < 0.01$). While the results of counted CFU were generally in agreement with the macroscopic evaluation of biofilm formation (Fig. SI4†), there was one exception: visual inspection revealed that the biofilm on the *iUV-PDMS*-coated coupons was clearly the most pronounced after the reference. Even after the biofilm was removed by rinsing, a slightly milky top layer was visible, which can be attributed to the strong attachment of the cells. Thus, incomplete biofilm removal may result in comparatively low values of CFU determination. Therefore, *iUV-PDMS* is the least suitable coating to prevent biofilms of this organism, which is in line with the poorer performance of this coating in the field studies and the electrochemistry experiments. For the uncoated reference, complete removal of the biofilm was also difficult (Fig. SI4†). However, this incomplete removal only leads to an underestimation of the adhering microbial counts, so the positive effect of the coatings tends to be underestimated and the reduction of biofouling is even more pronounced.

The effect of the different coatings on the biofilm formation of *P. fluorescens* was also investigated. In contrast to those of *T. thioparus*, the biofilms formed by these bacteria were easily removed from all coupons (Fig. SI5†). As summarized in Fig. 5b, the number of surface-attached cells was reduced by the different coatings around 50%. Apart from the *iTuSu* coating ($p = 0.056$), all reductions were statistically significant ($p < 0.05$). We suspect that the comparatively weaker effect of the coatings against *P. fluorescens* could be due to the well-known production of surface-active molecules by this organism.[70] The secreted biosurfactants could change the surface chemistry of the

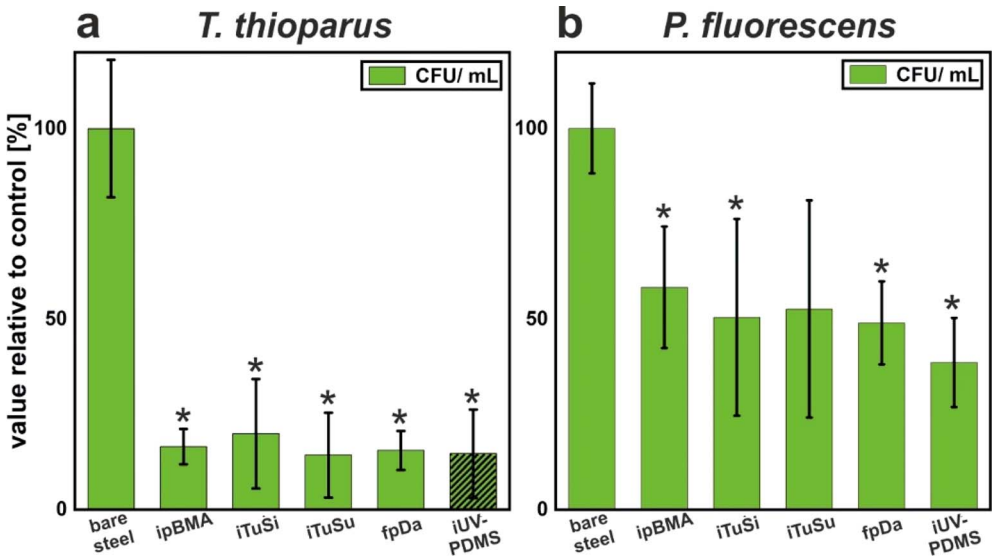

Fig. 5 Bacterial attachment on carbon steel substrates coated with different liquid-infused coatings. The number of cells attached to the substrates was evaluated *via* the counting of colony-forming units (CFUs). All values represent the mean ± SD from triplicate experiments and are shown relative to the uncoated reference. (a) *Thiobacillus thioparus*. Values that are significantly different from the bare steel control are marked with an asterisk (*) ($p < 0.05$). The value for *iUV-PDMS* is shown as a shaded bar because it is underestimated due to the incomplete detachment of the biofilm from the coupon. (b) *Pseudomonas fluorescens*. Values that are significantly different from the bare steel control are marked with an asterisk (*) ($p < 0.01$).

coatings and thus compromise their repellency properties, leading to less pronounced biofilm prevention.

Although the extent of biofilm prevention differed between the two organisms, it is encouraging that the developed liquid-infused coatings outperformed the reference in both cases, suggesting that certain physicochemical properties of surfaces may impede the attachment of different bacterial groups. This is important since biofilms are usually composed of various microorganisms, which can also assist each other in adhering to a particular substrate. By producing adhesive molecules and inducing intercellular interactions, the coexistence of multiple species within a biofilm is promoted.[71] Successful coating strategies should therefore ideally prevent or at least delay the attachment of various types of organisms.

Conclusions

In conclusion, we investigated the performance of a set of liquid-infused coatings with low environmental impact against biofouling in different freshwater environments. We combined field studies with long-term exposure over several months with laboratory experiments under defined conditions to probe the performance against corrosion and bacterial colonialization. In both field studies, liquid-infused coatings outperformed the uncoated references. The different types of liquid-infused coatings showed large variations in biofouling reduction, indicating that the design of the coating, *i.e.*, surface roughness, involved interfacial energies, and adhesion to the substrate, critically affects the performance. Noteworthily, liquid-infused coatings showed an improved performance under long-term exposure compared to the time-resolved field study. This demonstrates that the repeated exposure to liquid menisci upon removal of the samples from the water can be detrimental to their performance, presumably because the lubricant layer is continuously reduced by the air/water interface passing over the sample. The performance against corrosion of the different coatings broadly correlated with the reduction in biofouling, indicating that an intact lubricant layer prevents access to both (corrosive) ions and larger fouling species. The microbial attachment of different bacterial species known to be involved in microbially induced corrosion showed more heterogeneous results. While liquid-infused coatings efficiently prevented the attachment of *Thiobacillus thioparus*, in line with the reduced corrosion observed in the field studies, the performance against *Pseudomonas fluorescens* attachment was less pronounced. These results indicate that certain microbial species may be able to destabilize liquid-infused properties, possibly by modifying the involved surface chemistries. Overall, our results demonstrate the potential of environmentally benign liquid-infused coatings to reduce biofouling (and microbially induced corrosion) in freshwater systems. The study also showcases the current limitations of such coatings. Application scenarios with changing water levels and periodic exposure to changing water levels are problematic, because of the loss of lubricant *via* liquid menisci, which causes both a lack of performance and the loss of lubricant into the environment. A further aspect not addressed in this current study is the mechanical properties of the coatings, which can cause loss of performance by mechanical damage upon operation. These aspects are particularly critical for organogel-based coatings such as infused PDMS because of their inherently soft nature. The coating using sunflower oil as a lubricant rapidly failed in the field study, possibly due to its less hydrophobic nature. Finding a renewable alternative to persistent silicone oil as an

efficient lubricant in such coatings therefore remains an important challenge in the design of functional, sustainable repellent coatings.

Conflicts of interest

There are no conflicts to declare.

Acknowledgements

This study was funded by the Bavarian Ministry for the Environment and Consumer Protection and the Bavarian Environment Agency. T. A. B. thanks the DFG (grant number 442826449) for financial support. N. V. acknowledges support by the Deutsche Forschungsgemeinschaft (DFG) under grant number VO 1824/9-1.

References

1 G. Jones, in *Advances in Marine Antifouling Coatings and Technologies*, Woodhead Publishing, 2009, pp. 19–45.
2 K. A. Dafforn, J. A. Lewis and E. L. Johnston, *Mar. Pollut. Bull.*, 2011, **62**, 453–465.
3 R. Deng, T. Shen, H. Chen, J. Lu, H. C. Yang and W. Li, *J. Mater. Chem. A*, 2020, **8**, 7536–7547.
4 M. E. Callow and J. A. Callow, *Biologist*, 2002, **49**, 10–14.
5 M. A. Champ, *Sci. Total Environ.*, 2000, **258**, 21–71.
6 Y. K. Demirel, D. Uzun, Y. Zhang, H. C. Fang, A. H. Day and O. Turan, *Biofouling*, 2017, **33**, 819–834.
7 M. P. Schultz, J. A. Bendick, E. R. Holm and W. M. Hertel, *Biofouling*, 2011, **27**, 87–98.
8 B. J. Little, D. J. Blackwood, J. Hinks, F. M. Lauro, E. Marsili, A. Okamoto, S. A. Rice, S. A. Wade and H. C. Flemming, *Corros. Sci.*, 2020, **170**, 108641.
9 P. Perego and B. Fabiano, in *Encyclopedia of Industrial Biotechnology: Bioprocess, Bioseperation, and Cell Technology*, John Wiley & Sons, Inc., 2009, pp. 1–21.
10 D. Enning and J. Garrelfs, *Appl. Environ. Microbiol.*, 2014, **80**, 1226–1236.
11 D. Xu, T. Gu and D. R. Lovley, *Nat. Rev. Microbiol.*, 2023, **21**, 705–718.
12 Y. Jin, E. Zhou, T. Ueki, D. Zhang, Y. Fan, D. Xu, F. Wang and D. R. Lovley, *Angew. Chem., Int. Ed.*, 2023, **62**, 1–9.
13 E. Zhou, F. Li, D. Zhang, D. Xu, Z. Li, R. Jia, Y. Jin, H. Song, H. Li, Q. Wang, J. Wang, X. Li, T. Gu, A. M. Homborg, J. M. C. Mol, J. A. Smith, F. Wang and D. R. Lovley, *Water Res.*, 2022, **219**, 118553.
14 B. D. James, K. M. Kimmins, M. T. Nguyen, A. J. Lausch and E. D. Sone, *Sci. Rep.*, 2021, **11**, 1–10.
15 A. Lacoursière-Roussel, D. G. Bock, M. E. Cristescu, F. Guichard and C. W. McKindsey, *Biol. Invasions*, 2016, **18**, 3681–3695.
16 M. Ożgo, M. Urbańska, P. Hoos, H. K. Imhof, M. Kirschenstein, J. Mayr, F. Michl, R. Tobiasz, M. von Wesendonk, S. Zimmermann and J. Geist, *Ecol. Evol.*, 2020, **10**, 4918–4927.
17 C. S. Elton, *The Ecology of Invasions by Animals and Plants*, Springer Nature, 2020.
18 D. L. Strayer, *Front. Ecol. Environ.*, 2009, **7**, 135–141.
19 N. A. Connelly, C. R. O'Neill, B. A. Knuth and T. L. Brown, *Environ. Manage.*, 2007, **40**, 105–112.
20 L. Petrone, A. Kumar, C. N. Sutanto, N. J. Patil, S. Kannan, A. Palaniappan, S. Amini, B. Zappone, C. Verma and A. Miserez, *Nat. Commun.*, 2015, **6**, 8737.
21 H. G. Silverman and F. F. Roberto, *Mar. Biotechnol.*, 2007, **9**, 661–681.
22 B. K. Ahn, *J. Am. Chem. Soc.*, 2017, **139**, 10166–10171.
23 J. D. Gu, in *Handbook of Environmental Degradation of Materials*, William Andrew Inc., 2005, pp. 179–206.
24 R. F. Lee, *Mar. Environ. Res.*, 1991, **32**, 29–35.
25 B. Antizar-Ladislao, *Environ. Int.*, 2008, **34**, 292–308.
26 L. Vimercati, D. Cavone, A. Caputi, L. De Maria, M. Tria, E. Prato and G. M. Ferri, *Front. Public Heal.*, 2020, **8**, 1–19.
27 B. Zhang and W. Xu, *New J. Chem.*, 2021, **45**, 15170–15179.
28 S. Sunny, G. Cheng, D. Daniel, P. Lo, S. Ochoa, C. Howell, N. Vogel, A. Majid and J. Aizenberg, *Proc. Natl. Acad. Sci. U. S. A.*, 2016, **113**, 11676.
29 D. C. Leslie, A. Waterhouse, J. B. Berthet, T. M. Valentin, A. L. Watters, A. Jain, P. Kim, B. D. Hatton, A. Nedder, K. Donovan, E. H. Super, C. Howell, C. P. Johnson, T. L. Vu, D. E. Bolgen, S. Rifai, A. R. Hansen, M. Aizenberg, M. Super, J. Aizenberg and D. E. Ingber, *Nat. Biotechnol.*, 2014, **32**, 1134–1140.
30 N. MacCallum, C. Howell, P. Kim, D. Sun, R. Friedlander, J. Ranisau, O. Ahanotu, J. J. Lin, A. Vena, B. Hatton, T.-S. Wong and J. Aizenberg, *ACS Biomater. Sci. Eng.*, 2015, **1**, 43–51.
31 A. K. Epstein, T.-S. Wong, R. A. Belisle, E. M. Boggs and J. Aizenberg, *Proc. Natl. Acad. Sci. U. S. A.*, 2012, **109**, 13182–13187.
32 S. Amini, S. Kolle, L. Petrone, O. Ahanotu, S. Sunny, C. N. Sutanto, S. Hoon, L. Cohen, J. C. Weaver, J. Aizenberg, N. Vogel and A. Miserez, *Science*, 2017, **357**, 668–673.
33 K. M. Kimmins, B. D. James, M. T. Nguyen, B. D. Hatton and E. D. Sone, *ACS Appl. Bio Mater.*, 2019, **2**, 5841–5847.
34 S. Basu, B. M. Hanh, J. Q. Isaiah Chua, D. Daniel, M. H. Ismail, M. Marchioro, S. Amini, S. A. Rice and A. Miserez, *J. Colloid Interface Sci.*, 2020, **568**, 185–197.
35 S. Kolle, O. Ahanotu, A. Meeks, S. Stafslien, M. Kreder, L. Vanderwal, L. Cohen, G. Waltz, C. S. Lim, D. Slocum, E. M. Greene, K. Hunsucker, G. Swain, D. Wendt, S. L. M. Teo and J. Aizenberg, *Sci. Rep.*, 2022, **12**, 1–13.
36 L. Xiao, J. Li, S. Mieszkin, A. Di Fino, A. S. Clare, M. E. Callow, J. A. Callow, M. Grunze, A. Rosenhahn, P. A. Levkin and U. K. Birmingham, *ACS Appl. Mater. Interfaces*, 2013, **5**, 10074–10080.
37 T. S. Wong, S. H. Kang, S. K. Y. Tang, E. J. Smythe, B. D. Hatton, A. Grinthal and J. Aizenberg, *Nature*, 2011, **477**, 443–447.
38 M. Villegas, Y. Zhang, N. Abu Jarad, L. Soleymani and T. F. Didar, *ACS Nano*, 2019, **13**, 8517–8536.

39 D. J. Preston, Y. Song, Z. Lu, D. S. Antao and E. N. Wang, *ACS Appl. Mater. Interfaces*, 2017, **9**, 42383–42392.
40 J. Lee, J. Yoo, J. Kim, Y. Jang, K. Shin, E. Ha, S. Ryu, B. G. Kim, S. Wooh and K. Char, *ACS Appl. Mater. Interfaces*, 2019, **11**, 6550–6560.
41 N. Vogel, R. A. Belisle, B. Hatton, T. S. Wong and J. Aizenberg, *Nat. Commun.*, 2013, **4**, 1–10.
42 S. Wooh and H.-J. Butt, *Angew. Chem.*, 2017, **129**, 5047–5051.
43 X. Yao, S. S. Dunn, P. Kim, M. Duffy, J. Alvarenga and J. Aizenberg, *Angew. Chem., Int. Ed.*, 2014, **53**, 4418–4422.
44 B. Yi, S. Wang, C. Hou, X. Huang, J. Cui and X. Yao, *Chem. Eng. J.*, 2021, **405**, 127023.
45 S. Wooh and D. Vollmer, *Angew. Chem., Int. Ed.*, 2016, **55**, 6822–6824.
46 S. Chiera, C. Bittner and N. Vogel, *Adv. Mater. Interfaces*, 2021, **8**, 2100156.
47 S. Chiera, V. M. Koch, G. Bleyer, T. Walter, C. Bittner, J. Bachmann and N. Vogel, *ACS Appl. Mater. Interfaces*, 2022, **14**, 16735–16745.
48 K. E. Dehm, T. Walter, M. Weichselgartner, R. W. Crisp, K. Wommer, M. Aust and N. Vogel, *Adv. Mater. Interfaces*, 2023, **10**, 2202032.
49 A. B. Tesler, L. H. Prado, I. Thievessen, A. Mazare, P. Schmuki, S. Virtanen and W. H. Goldmann, *ACS Appl. Mater. Interfaces*, 2022, **14**, 29386–29397.
50 T. Walter, T. Hein, M. Weichselgartner, K. Wommer, M. Aust and N. Vogel, *Green Chem.*, 2022, **24**, 3009–3016.
51 J. LaCombe Barron and D. R. Lueking, *Appl. Environ. Microbiol.*, 1990, **56**, 2801–2806.
52 S. Peppou-Chapman, J. K. Hong, A. Waterhouse and C. Neto, *Chem. Soc. Rev.*, 2020, **49**, 3688–3715.
53 C. Howell, T. L. Vu, J. J. Lin, S. Kolle, N. Juthani, E. Watson, J. C. Weaver, J. Alvarenga and J. Aizenberg, *ACS Appl. Mater. Interfaces*, 2014, **6**, 13299–13307.
54 F. Schellenberger, J. Xie, N. Encinas, A. Hardy, M. Klapper, P. Papadopoulos, H. J. Butt and D. Vollmer, *Soft Matter*, 2015, **11**, 7617–7626.
55 H. H. Tran, D. Lee and D. Riassetto, *Rep. Prog. Phys.*, 2023, **86**, 066601.
56 M. Tress, S. Karpitschka, P. Papadopoulos, J. H. Snoeijer, D. Vollmer and H. J. Butt, *Soft Matter*, 2017, **13**, 3760–3767.
57 P. Baumli, M. D'Acunzi, K. I. Hegner, A. Naga, W. S. Y. Wong, H. J. Butt and D. Vollmer, *Adv. Colloid Interface Sci.*, 2021, **287**, 102329.
58 S. Peppou-Chapman and C. Neto, *Langmuir*, 2021, **37**, 3025–3037.
59 S. Sunny, N. Vogel, C. Howell, T. L. Vu and J. Aizenberg, *Adv. Funct. Mater.*, 2014, **24**, 6658–6667.
60 A. B. Tesler, L. H. Prado, M. M. Khusniyarov, I. Thievessen, A. Mazare, L. Fischer, S. Virtanen, W. H. Goldmann and P. Schmuki, *Adv. Funct. Mater.*, 2021, **31**, 2101090.
61 L. H. Prado, D. Böhringer, A. Mazare, L. Sotelo, G. Sarau, S. Christiansen, B. Fabry, P. Schmuki, S. Virtanen, W. H. Goldmann and A. B. Tesler, *ACS Appl. Mater. Interfaces*, 2023, **15**, 31776–31786.
62 E. McCafferty, *Introduction to Corrosion Science*, Springer Science+Business Media, New York, 2010.
63 T. My, P. Nguyen, X. Sheng, Y.-P. Ting and S. O. Pehkonen, *Ind. Eng. Chem. Res.*, 2008, **47**, 4703–4711.
64 G. Płaza and V. Achal, *Int. J. Mol. Sci.*, 2020, **21**, 2152.
65 A. J. Spark, D. W. Law, L. P. Ward, I. S. Cole and A. S. Best, *Environ. Sci. Technol.*, 2017, **51**, 8501–8509.
66 M. Boretska and S. Bellenberg, *J. Microb. Biochem. Technol.*, 2013, **5**, 068–073.
67 M. Okazaki, T. Sugita, M. Shimizu, Y. Ohode, K. Iwamoto, E. W. De Vrind-de Jong, J. P. M. De Vrind and P. L. A. M. Corstjens, *Appl. Environ. Microbiol.*, 1997, **63**, 4793–4799.
68 R. Amendola and A. Acharjee, *Front. Microbiol.*, 2022, **13**, 806688.
69 C. Wilson, R. Lukowicz, S. Merchant, H. Valquier-Flynn, J. Caballero, J. Sandoval, M. Okuom, C. Huber, T. Durham Brooks, E. Wilson, B. Clement, C. D. Wentworth and A. E. Holmes, *Res. Rev.: J. Eng. Technol.*, 2017, **6**(4), 1–25.
70 L. Bunster, N. J. Fokkema and B. Schippers, *Appl. Environ. Microbiol.*, 1989, **55**, 1340–1345.
71 A. Luo, F. Wang, D. Sun, X. Liu and B. Xin, *Front. Microbiol.*, 2022, **12**, 757327.